JOURNAL OF GEOPHYSICAL RESEARCH, VOL. 97, NO. B5, PAGES 6643-6659, MAY 10, 1992

A COMPARATIVE STUDY OF SCATTERING, INTRINSIC,AND CODA Q^{-1} FOR HAWAII, LONG VALLEY, AND CENTRAL CALIFORNIA BETWEEN 1.5 AND 15.0 HZ

Kevin Mayeda[1] and Stuart Koyanagi[2]

Department of Geological Sciences, University of Southern California, Los Angeles

Mitsuyuki Hoshiba

Meteorological Research Institute, Tsukuba, Japan

Keiiti Aki and Yuehua Zeng[3]

Department of Geological Sciences, University of Southern California, Los Angeles

Abstract. A new method recently developed by Hoshiba et al. [1991] was used to separate the effects of scattering Q^{-1} and intrinsic Q^{-1} from an analysis of the S wave and its coda in Hawaii, Long Valley, and central California. Unlike the method of Wu [1985], which involves integration of the entire S wave energy, the new method relies on the integration of the S wave energy for three successive time windows as a function of hypocentral distance. Using the fundamental separability of source, site, and path effects for coda waves, we normalized the energy in each window for many events recorded at many stations to a common site and source. We plotted the geometric spreading-corrected normalized energy as a function of hypocentral distance. The data for all three time windows were then simultaneously fit to Monte Carlo simulations assuming isotropic body wave scattering in a medium of randomly and uniformly distributed scatterers and uniform intrinsic Q^{-1}. In general, for frequencies less than or equal to 6.0 Hz, scattering Q^{-1} was greater than intrinsic Q^{-1}, whereas above 6.0 Hz the opposite was true. Model fitting was quite good for frequencies greater than or equal to 6.0 Hz at all distances, despite the model's simplicity. The small range in energy values for any particular time window demonstrates that the site effect can be effectively stripped away using the coda method. Though the model fitting generally worked for 1.5 and 3.0 Hz, the model has difficulty in fitting the whole distance range simultaneously, especially at short distances. Despite the poor fit at low frequency, the results generally support that in all three regions the scattering Q^{-1} is strongly frequency dependent, decreasing proportional to frequency or faster, whereas intrinsic Q^{-1} is considerably less frequency dependent. This suggests that the scale length of heterogeneity responsible for scattering is at least comparable to the wavelength for the lowest frequencies studied, of the order of a few kilometers. The lithosphere studied in all three regions can be characterized as a random medium with velocity fluctuation characterized by exponential or Gaussian autocorrelation functions which predict scattering Q^{-1} decreasing proportional to frequency or faster. For all frequencies the observed coda Q^{-1} is intermediate between the total Q^{-1} and expected coda Q^{-1} in contrast with theoretical results for an idealized case of uniform distribution of scatterers and homogeneous absorption which predict that coda Q^{-1} should be close to the intrinsic Q^{-1}. We will discuss possible causes for this discrepancy.

Introduction

The understanding of scattering attenuation has benefited recently by studying wave propagation through media with discrete cavities and inclusions [Benites, 1990] or through random media with velocity fluctuations [Wu, 1982; Sato, 1982; Frankel and Clayton, 1986]. The frequency-dependent scattering attenuation has been investigated using statistical models of the seismic velocity fluctuation, represented by its spatial autocorrelation function, and characterized usually as exponential, self-similar or Gaussian. Attenuation estimated from direct S waves [Aki, 1980; Rautian and Khalturin, 1978; Taylor et al., 1986] contain the combined effects of scattering and intrinsic loss. Attenuation inferred from the decay rate of the coda [Aki and Chouet, 1975; Rautian and Khalturin, 1978; Singh and Herrmann, 1983; Sato, 1988] is also a combination of scattering and intrinsic attenuation; however, both of these methods are incapable of separating these effects. The relative contributions to the apparent attenuation have been the subject of much interest [Aki, 1980; Frankel and Wennerberg, 1987]. The goal of this study is to separate the contributions to the apparent decay, namely, the intrinsic and scattering attenuation, Q_i^{-1} and Q_s^{-1}, where the total attenuation, Q_t^{-1} is given as

$$\frac{1}{Q_t} = \frac{1}{Q_s} + \frac{1}{Q_i} \tag{1}$$

and

$$Q_s^{-1} = k^{-1}\eta_s \quad Q_i^{-1} = k^{-1}\eta_i$$

where k is the wavenumber and η_s and η_i are the scattering and intrinsic attenuation coefficients, respectively. Wu's [1985] method, based on the radiative transfer theory [e.g., Ishimaru, 1978], allows an estimation of the relative amounts of scattering and intrinsic attenuation from the dependence of the entire S wave energy on hypocentral distance [Wu and Aki, 1988; Mayeda et al., 1991a; McSweeney et al., 1991; Toksöz et al., 1988]. Recently, Hoshiba et al. [1991] have developed a more reliable method, called "multiple lapse time window analysis", to estimate the scattering and intrinsic Q^{-1} by considering energy for three consecutive time windows as a function of hypocentral distance [Fehler et al., 1992]. We define the seismic albedo, $B_0 = \eta_s/(\eta_s + \eta_i)$ as the relative

[1]Now at Lawrence Livermore National Laboratory, Earth Sciences Department, Livermore, California.

[2]Now at National Earthquake Information Center, Denver, Colorado.

[3]Now at Department of Geological Sciences, University of Nevada, Reno.

Paper number 91JB03094.
0148-0227/92/91JB-03094$05.00

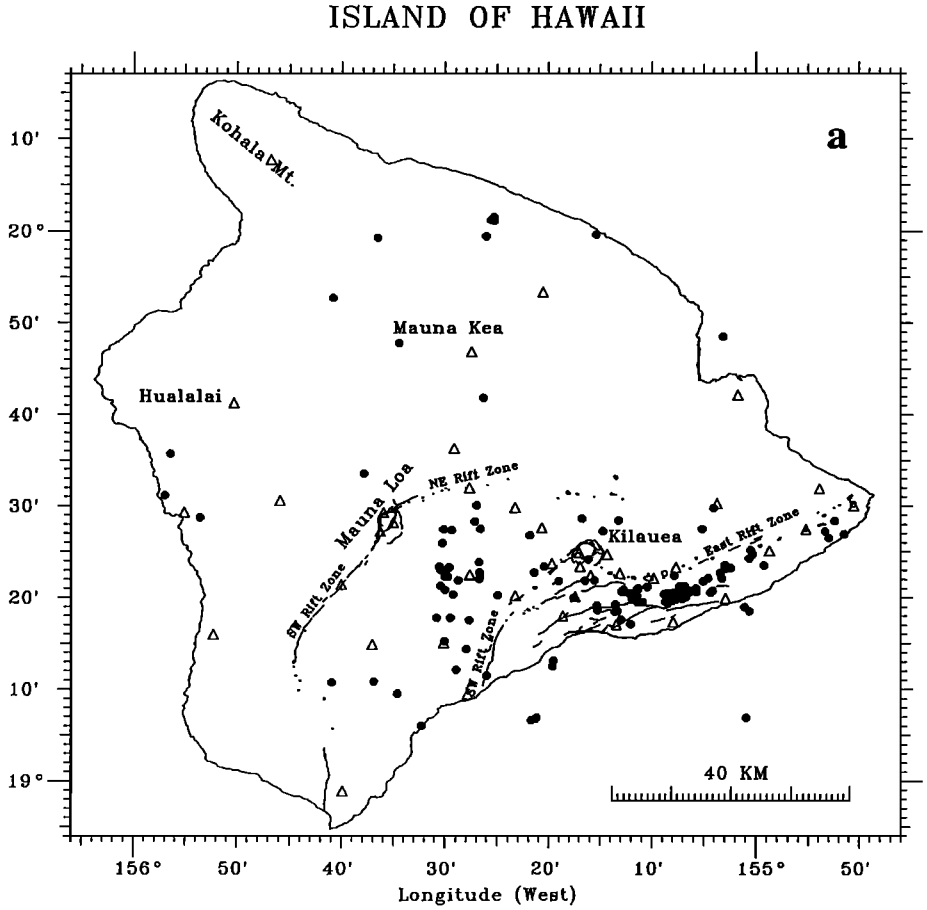

Fig. 1. Maps showing the distribution of events (circles) and stations (triangles) used in (a) Hawaii, (b) central California, and (c) Long Valley caldera. All waveform data were collected from the USGS seismic networks in northern California at Menlo Park and the Hawaiian Volcano Observatory, island of Hawaii.

amount of scattering attenuation to total attenuation and the total attenuation coefficient as L_e^{-1}, where $L_e = 1/(\eta_s + \eta_i)$ is the extinction distance over which the primary S wave energy is decreased by e^{-1}. When $B_0 > 0.5$, scattering attenuation is dominant, and when $B_0 < 0.5$, intrinsic loss is dominant. The shapes of the three energy curves as a function of source-receiver distance are simultaneously fit to Monte Carlo simulations using homogeneously distributed scatterers in a full space with uniform intrinsic attenuation under the assumption of isotropic multiple scattering for various B_0 and L_e [Hoshiba et al., 1991]. We shall apply Hoshiba et al.'s [1991] method to central California, Long Valley, California, and the island of Hawaii to obtain both the scattering and intrinsic Q^{-1} as a function of frequency. Resultant scattering and intrinsic Q^{-1} are then compared to observed coda Q^{-1} and expected coda Q^{-1} derived from the integral solution for multiple scattering by Zeng et al. [1991].

Data

Digital records of local earthquakes were collected from Long Valley, central California, and the island of Hawaii from the U.S. Geological Survey (USGS) seismic networks operated by their Menlo Park office and the Hawaiian Volcano Observatory. All events occurred from May 1987 and March 1990, with focal depths between five and 20 km and magnitudes ranging between 1.5 and 3.6. All records were from 1-Hz vertical seismometers and sampled at the rate of 100 samples per second. Instrument responses and gain settings were given by Nakata et al. [1987] for the Hawaii data and Eaton [1980] for the California data, all of which still apply to the current data set (J. Eaton, personal communication, 1990; J. Nakata, personal communication, 1990). Figure 1 shows the distribution of events and stations used in all three regions. All records chosen exhibited excellent signal to noise and were free from glitches or spurious signals.

Method

In order to apply Hoshiba et al.'s [1991] method, we need to obtain energy as a function of hypocentral distance for three successive time windows. First, we calculate for each seismogram the squared amplitude spectrum, $|F(\omega)|^2$ for three consecutive time windows defined at 0-15 s, 15-30 s, and 30-45 s measured from the onset of the S wave arrival, where ω is the angular frequency. Figure 2 shows representative seismograms from an event in the central California region along with the three time windows over which the measurement of energy was taken. To preserve the waveform of impulsive S wave arrivals, window tapers were not used in our fast Fourier transform (FFT) analysis. Best fitting model simulations to the observed data will then provide estimates of the scattering and intrinsic attenuation.

Coda Normalization to a Common Source and Site

Our normalization of all records to a common source and site is based on the empirically established fundamental separability of source, site, and path effect on coda waves [Aki, 1980; Phillips, 1985; Fehler et al., 1992; Mayeda et al.,

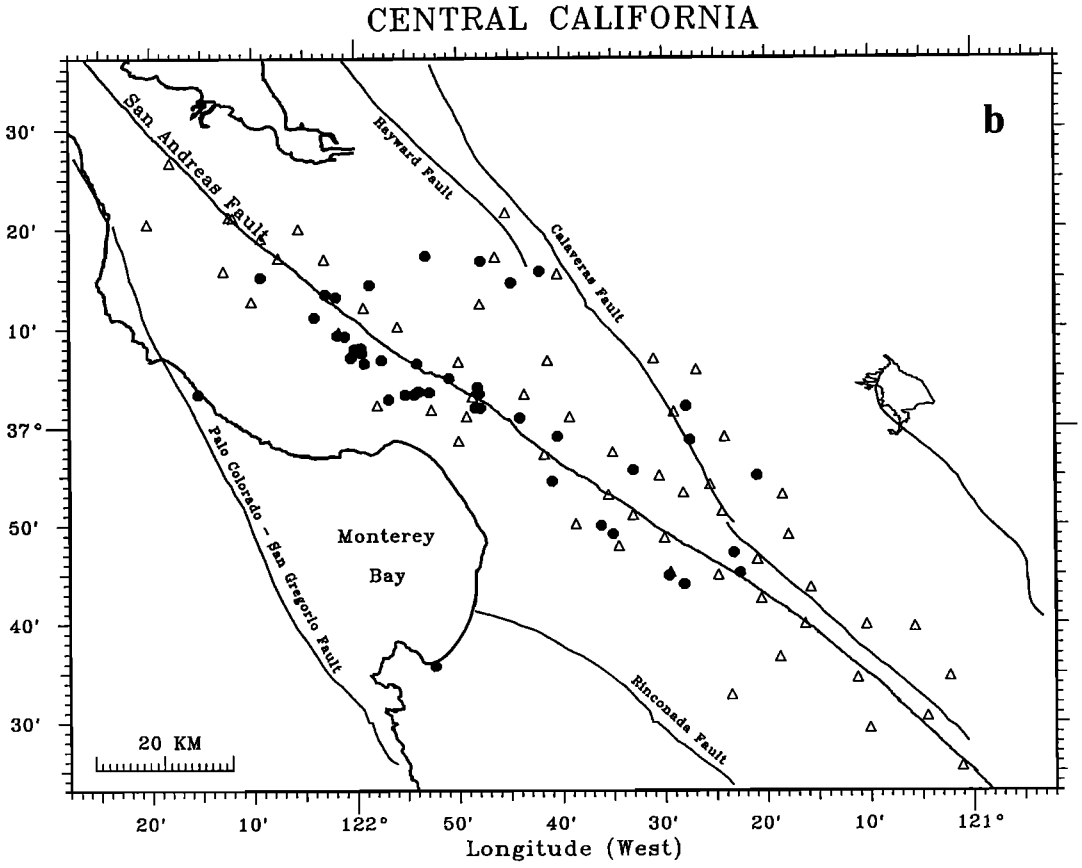

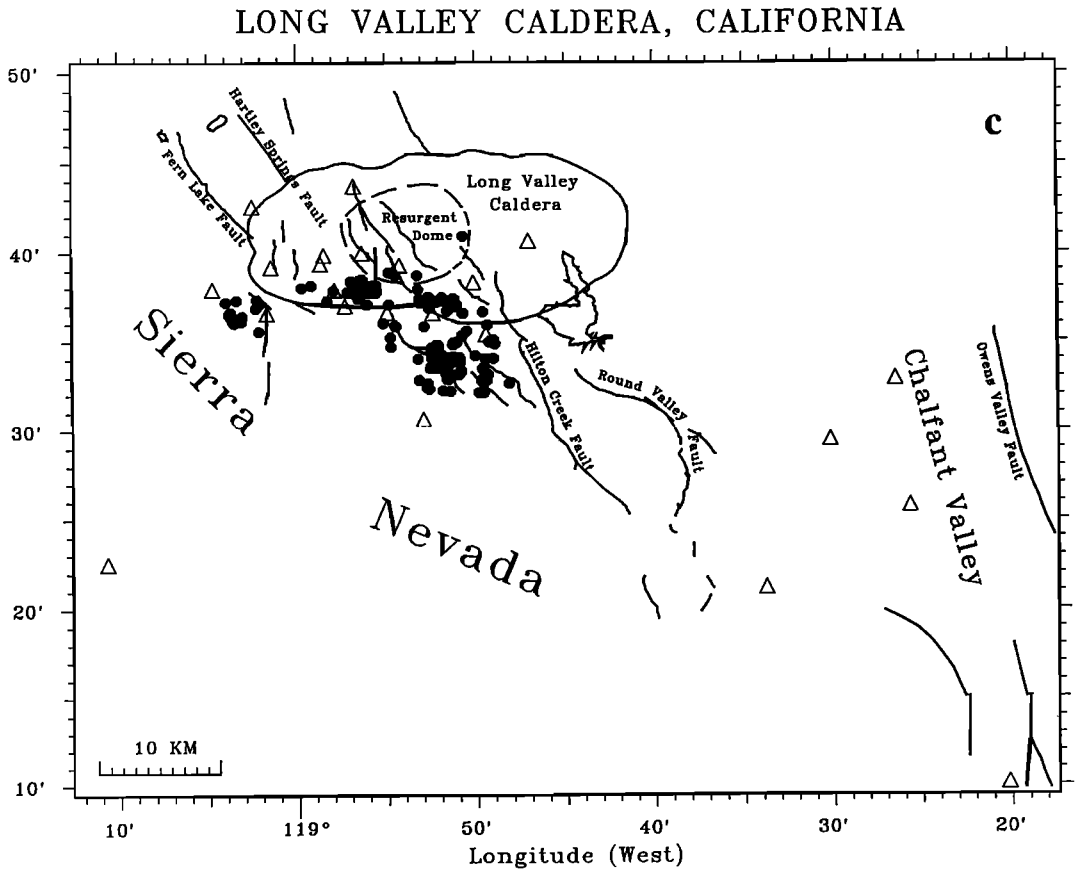

Fig. 1 (continued)

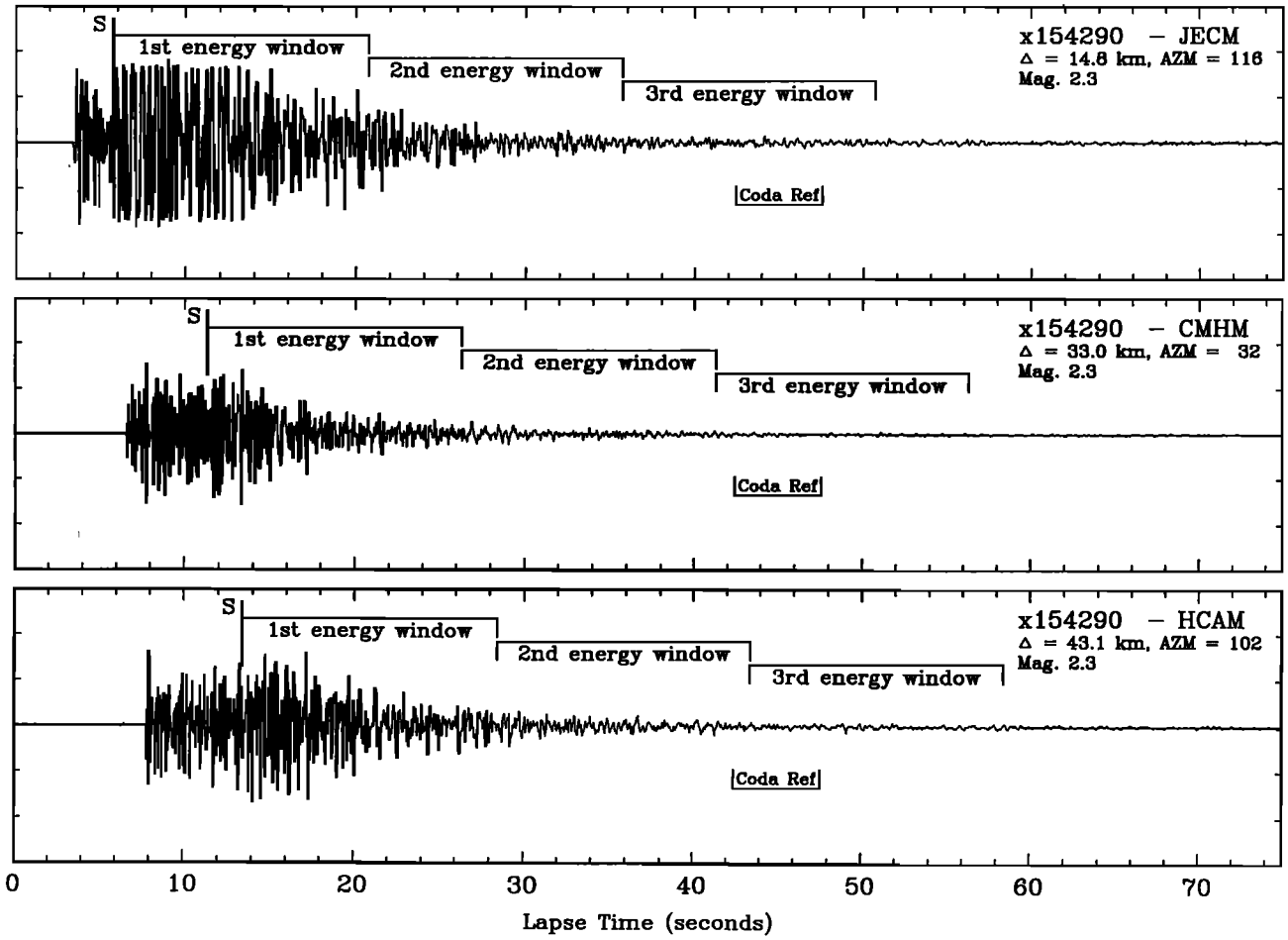

Fig. 2. Typical seismograms from an event in the central California region showing the three successive time windows for energy calculation and the reference coda window centered at 45 s lapse time. Clipped windows, such as the first window recorded at station JECM, were not processed.

1991b]. This is accomplished by dividing the energy in each window by the coda energy contained in a fixed reference time interval taken at later lapse times at least twice the S wave travel time.

Coda Energy in Space and Time

Though we assume the above fundamental separability of source, site, and path effects, a recent study by Koyanagi et al. [1992] on the island of Hawaii found the case in which it does not apply for frequencies lower than 6.0 Hz. They found that relative site amplification factors at any two stations were strongly dependent on the event distribution. If they used events in close proximity to one of the stations, other stations at considerably larger distances always underestimated the site amplification factor as compared to site amplification factors derived from events equidistant from the two stations. Fortunately, site amplification factors derived in their study relative to a reference station mainly consisted of events roughly equidistant from the two stations. Provided that the coda energy is isotropic about the source, site amplification factors derived from coda measured at the same lapse time and hypocentral distance from the source should represent the true site amplification factors. Koyanagi et al. [1992] demonstrated that single-station estimates of relative coda site amplification factor were identical to those derived using the average relative amplification over many stations. In their case, the coda site amplification factor at each station was made relative to the log average of at least 20 of the 40 stations in the array. Furthermore, they showed that the effect of inhomogeneously distributed coda energy did not affect their site amplification factors since the events they used were distributed roughly uniformly over the array.

Since the determination of B_0 and L_c depends critically on the shape of the energy curves as a function of source-receiver distance, we wished to find the distribution of coda energy in space. If the coda energy for a given lapse time window

Fig. 3. Site-effect corrected coda energy averaged over 10 km spacing on the island of Hawaii for all six frequency bands. The dashed lines represent coda energy at a lapse time of 20 s. Notice that for 1.5 and 3.0 Hz the coda energy is sharply decreasing with hypocentral distance, in contrast to the higher frequencies. The solid lines represent coda energy at 45 s lapse time. In general, the coda energy has become homogeneously distributed in space at this time, though the coda energy at 1.5 and 3.0 Hz decreases slightly with increasing hypocentral distance. This will cause the normalized energy estimates in each of the three time windows to be slightly overestimated at large distances.

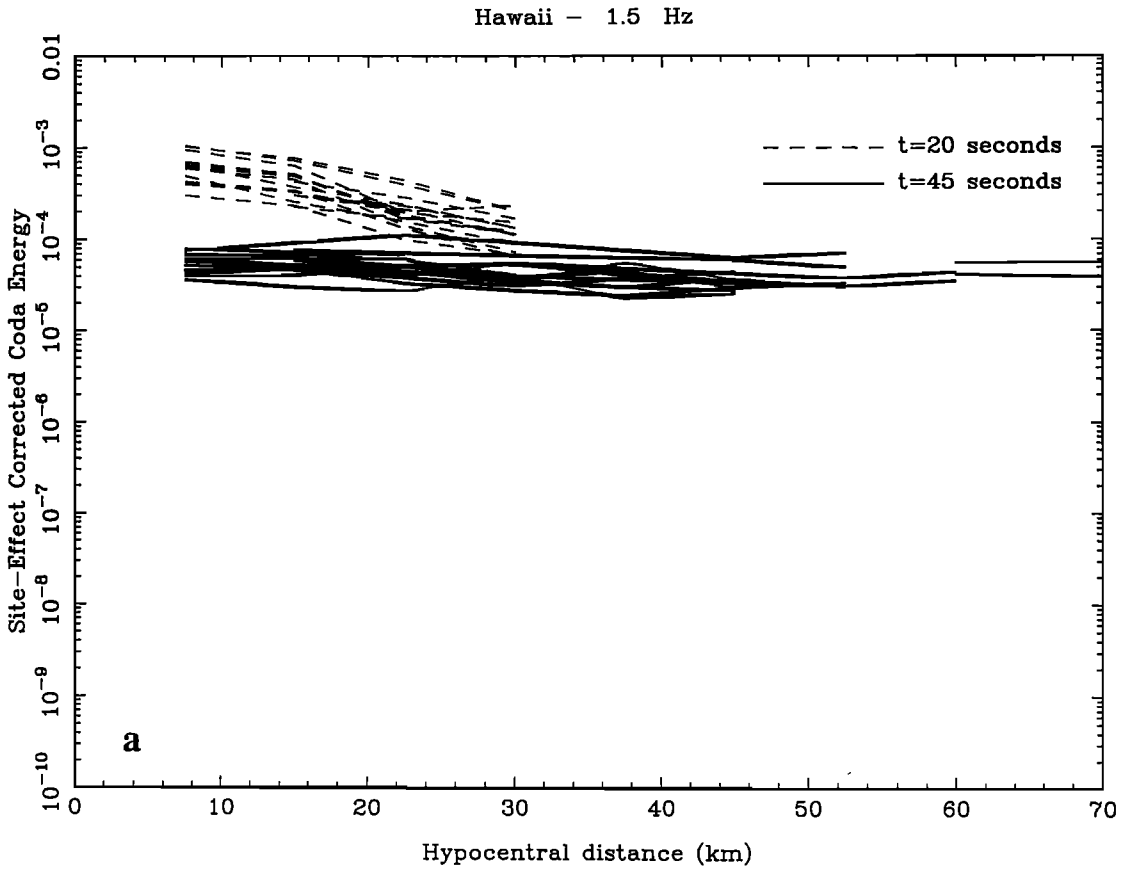

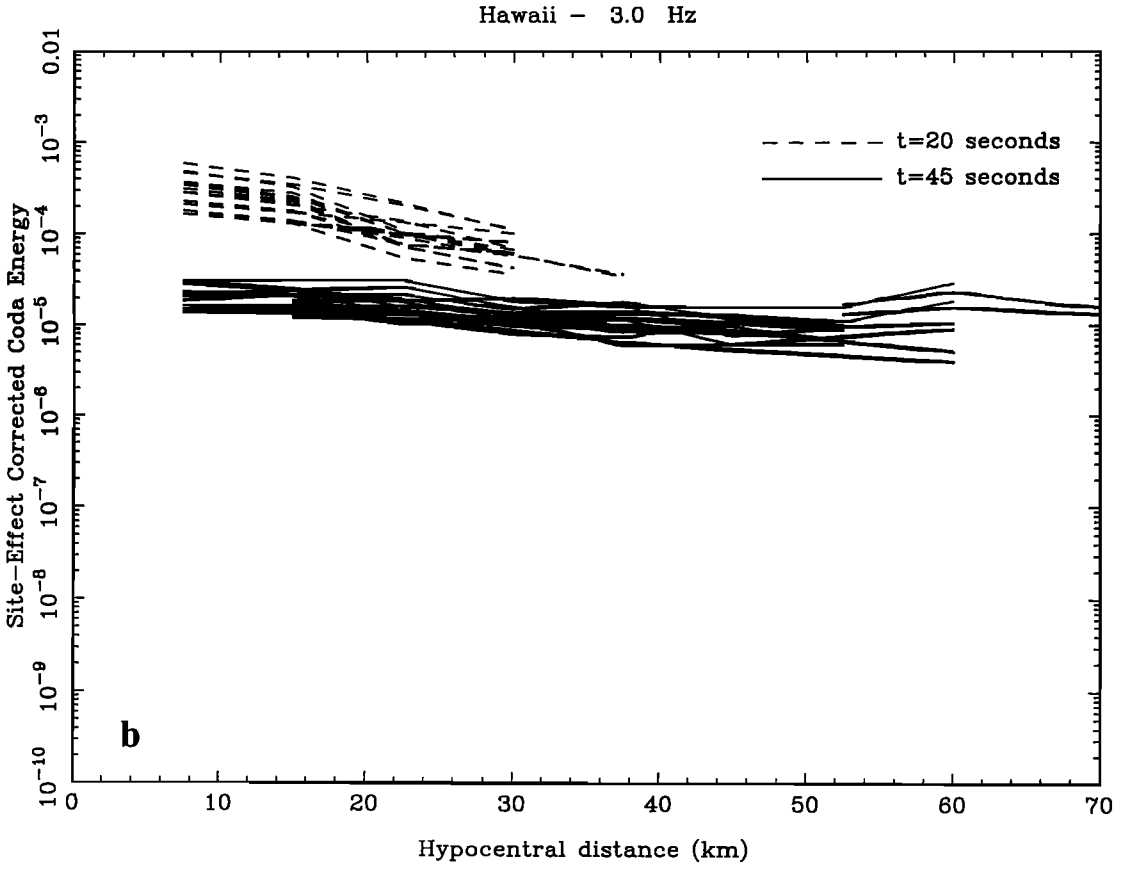

Fig. 3 (continued)

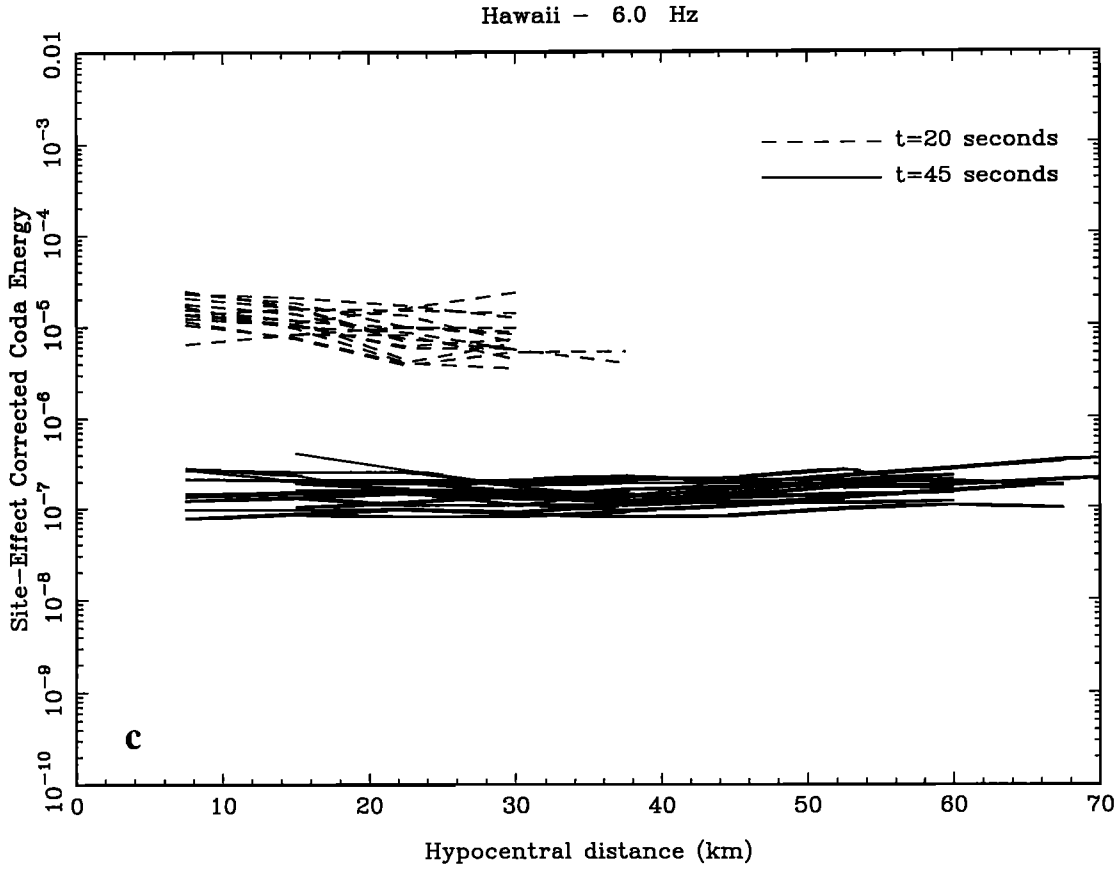

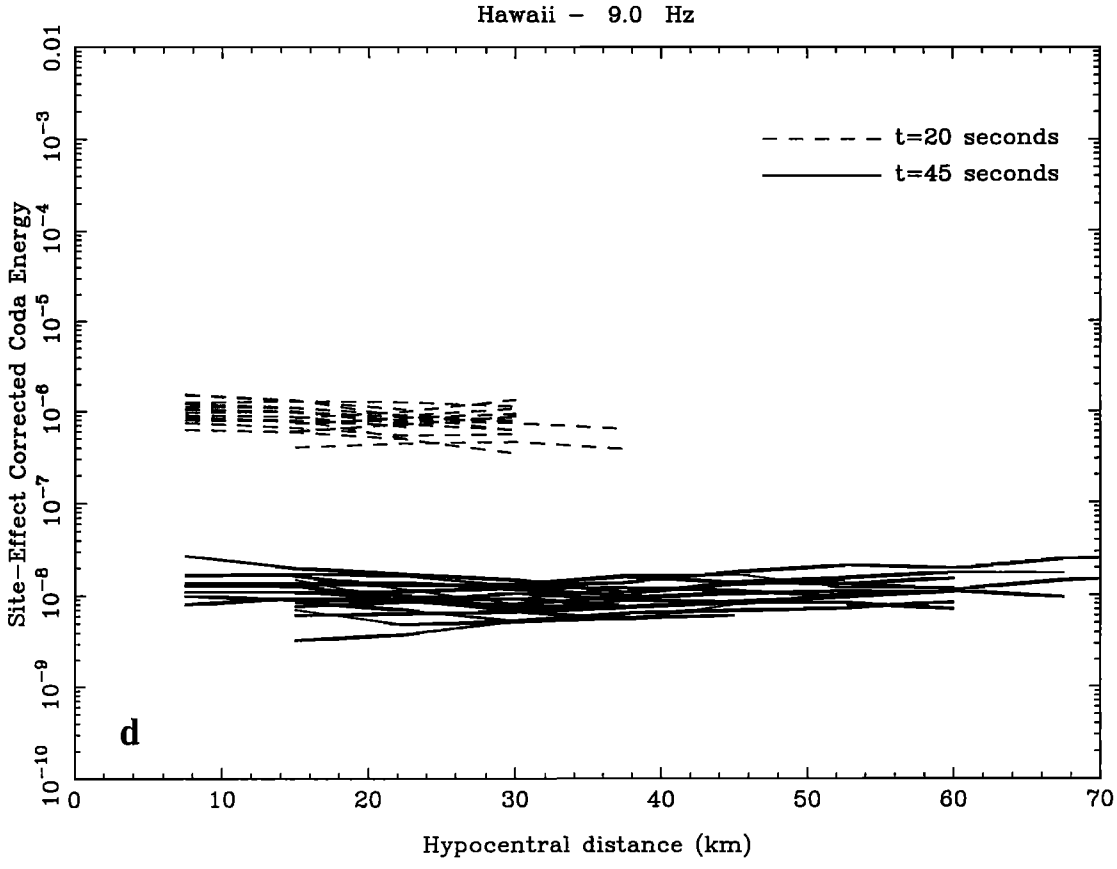

Fig. 3 (continued)

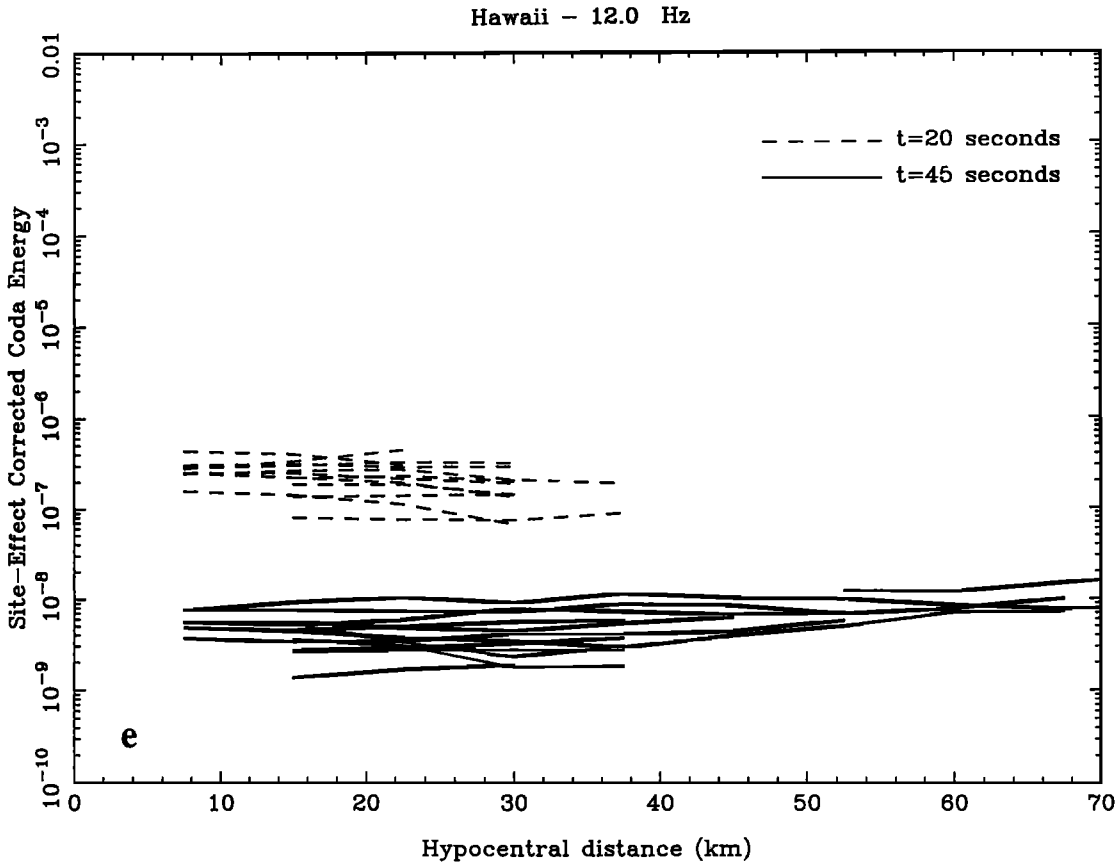

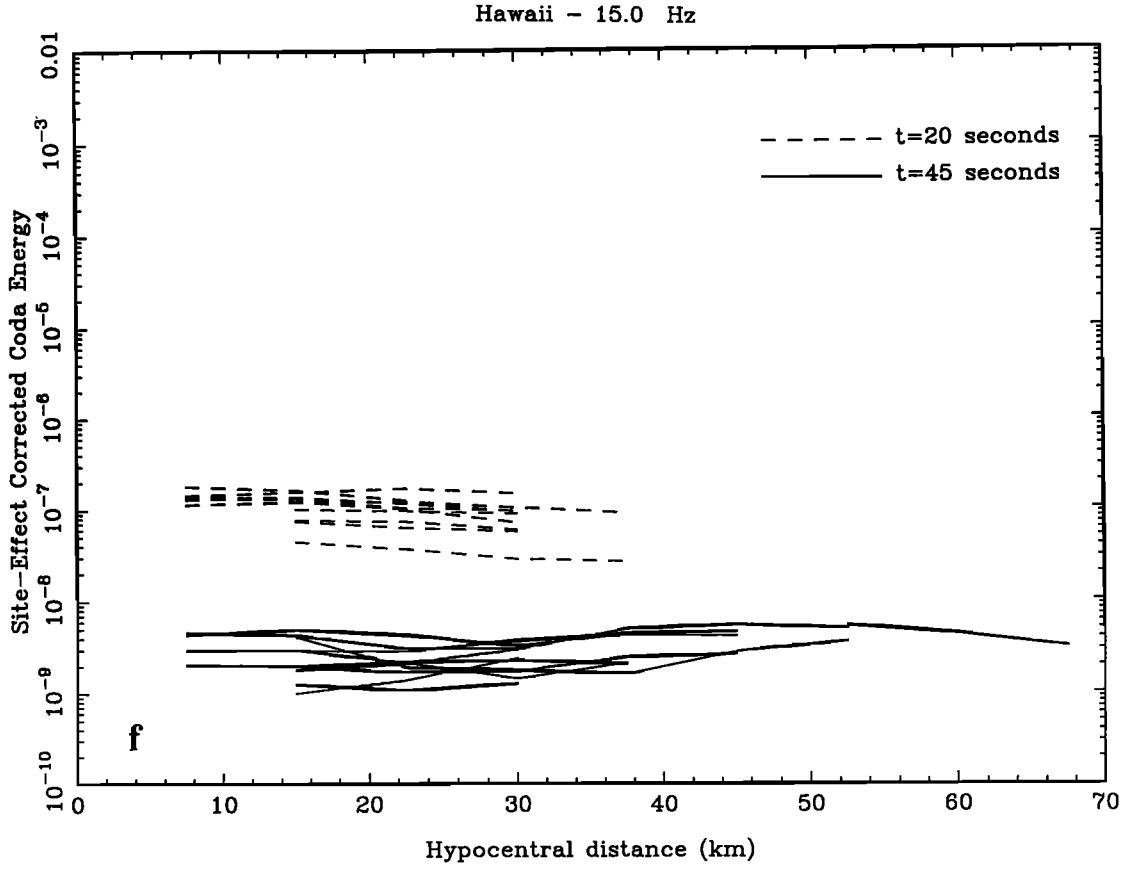

Fig. 3 (continued)

decreases significantly with increasing hypocentral distance, then normalization using the coda method will increasingly overestimate energy with larger hypocentral distances. We chose 10 events on the island of Hawaii with magnitudes between 2.7 and 2.8 which were well recorded by the Hawaiian Volcano Observatory network (HVO). Next, we divided the observed coda energy measured at each station by its corresponding site amplification factor from Koyanagi et al. [1992]. Figure 3 shows coda energy corrected for site effect over all frequencies plotted as a function of hypocentral distance for two lapse time windows, 20 s (dotted line) and 45 s (dashed line). The site-effect corrected coda energy measured at 20 s for the frequencies 1.5 and 3.0 Hz decreases significantly, roughly 80% in 30 km. However, at 45 s the coda energy only decreases by roughly 50% over 70 km. For frequencies above 3.0 Hz, the site-effect corrected coda energy is homogeneously distributed, even for the early lapse time. The coda window at 45 s lapse time was chosen because for all frequencies the site-effect corrected coda energy is roughly homogeneous. This observation justifies our use of the coda method for normalization to a common source and site for frequencies above 3.0 Hz, while for 1.5 and 3.0 Hz, the coda normalization to a common source and site will cause a slight overestimation in energy for each of the three time windows as hypocentral distance increases, roughly a factor of two in energy.

Observations

For our normalization to a common source and site, we chose a coda reference sample at 45 ± 2.5 s since as shown

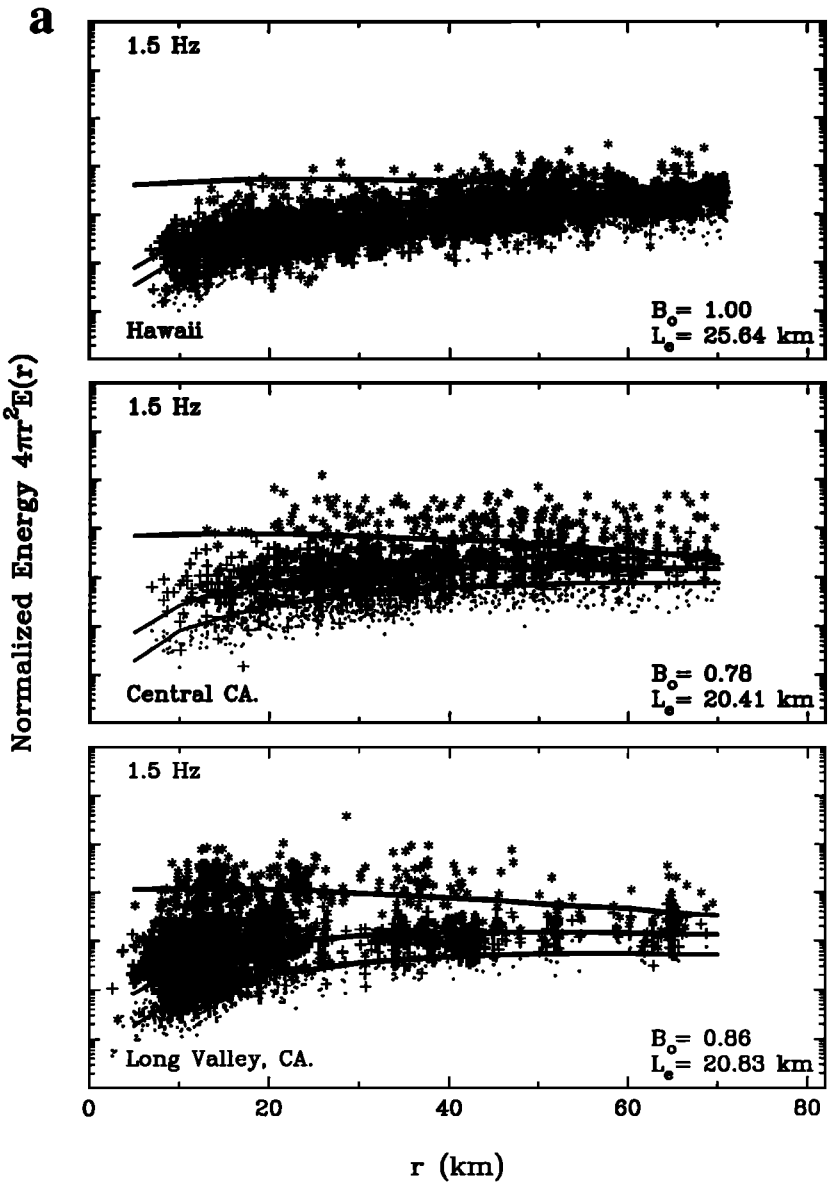

Fig. 4. Plots of normalized energy corrected for geometrical spreading for all three time windows, where (asterisks), (crosses), and (dots) represent energy measurements for the 0-15 s, 15-30 s and 30-45 s time windows, respectively. Notice that energy in the earliest time window for the Hawaii data at low frequencies (Figures 3a and 3b), increase up to at least 70 km hypocentral distance. This may be attributed to strong backscattering for Hawaii at these frequencies. Relative differences between the three time windows gives a qualitative measure of the degree of scattering. Solid lines are the best fit model estimates from the Monte Carlo simulations of Hoshiba et al. [1991]. The corresponding model parameters are listed in Table 1.

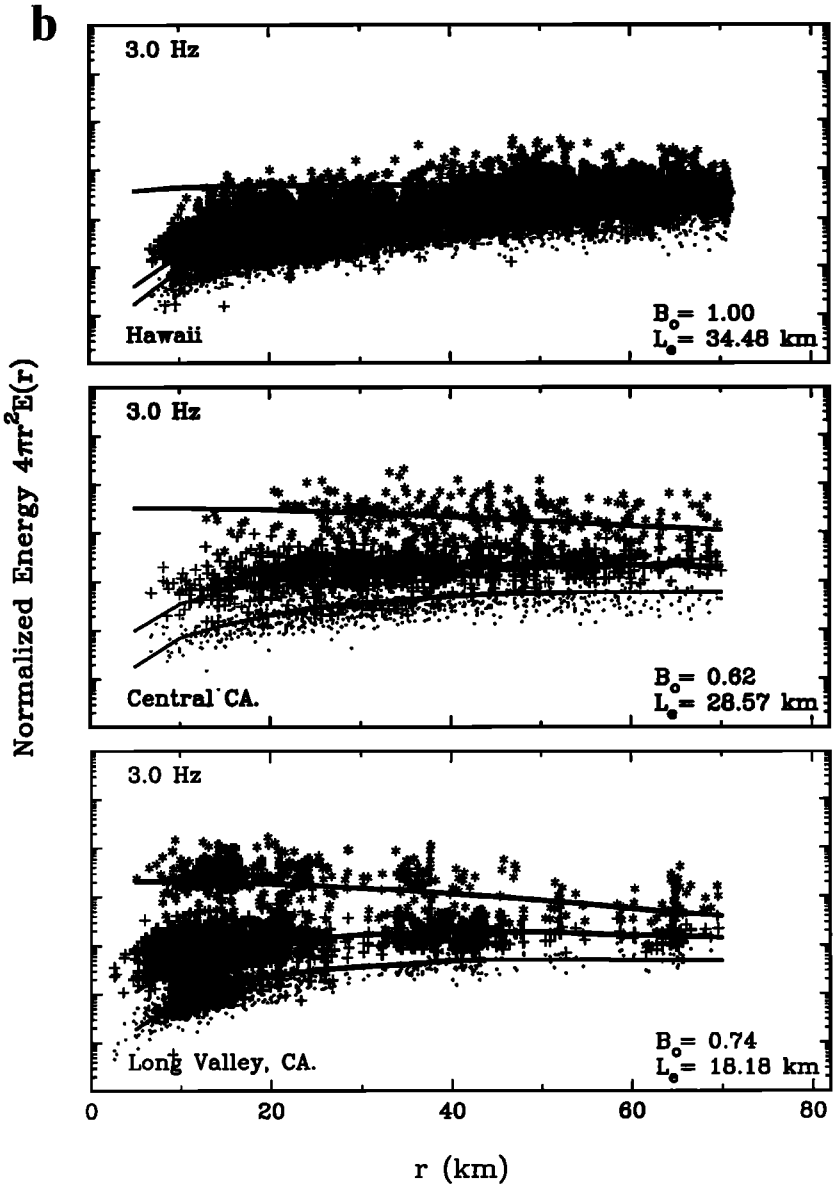

Fig. 4 (continued)

above the site-effect corrected coda energy is roughly homogeneous at this lapse time for all frequencies. The spectrum for each window and the coda reference was averaged over six frequency bands centered at 1.5, 3.0, 6.0, 9.0, 12.0, and 15.0 Hz, with bandwidths of ± 0.75 Hz for 1.5 Hz and ± 2.0 Hz for the remaining center frequencies. We eliminated the effect of ambient noise by taking a noise sample of the same length prior to the P wave arrival and subtracted the noise energy from the S wave energy in each time window as well as the coda reference sample. The data with signal power less than twice the noise were discarded. We can then plot the normalized energy, $E(\omega|r)$ given as,

$$E(\omega|r) = \frac{|F(\omega)|^2}{|F_{coda}(\omega)|^2} \quad (2)$$

where $|F(\omega)|^2$ is the energy for the first, second or third time window for a station at r kilometers hypocentral distance, and $|F_{coda}(\omega)|^2$ is the energy of the coda at the reference interval for the same trace. Next, we correct for geometrical spreading by multiplying $E(\omega|r)$ by the square of hypocentral distance to compare with Hoshiba et al.'s [1991] simulation. Figure 4 shows plots of normalized energy corrected for geometrical spreading versus hypocentral distance, r in kilometers, for all three regions and each frequency band. The small observed variability in the energy values for any particular time window is reassuring; this further supports the use of the coda method for normalization to a common site and source. The larger scatter observed for the earliest time window can be attributed to differences in source radiation pattern among the events, whereas the later two time windows, which comprise the later coda, show significantly less scatter [Fehler et al., 1992]. This is expected if coda waves are generated by scattering from many scatterers, thereby averaging the effect of the source radiation over all directions. In our case, application of the coda method effectively strips off the near surface effects of amplification and absorption, thereby normalizing all the events to a common source size. The energy plotted in Figure 4 represents scattered S wave energy in the lithosphere without near surface effects and essentially represents the energy in a homogeneous half-space.

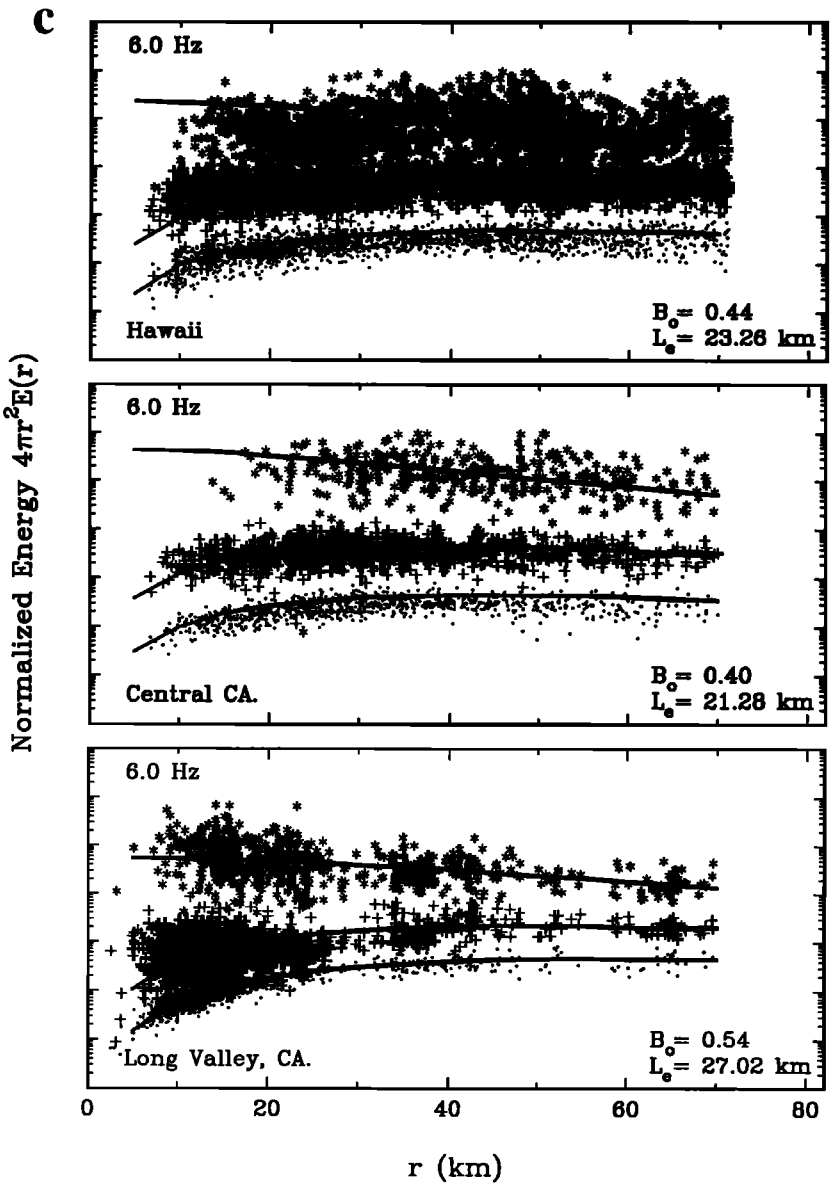

Fig. 4 (continued)

Results from Monte Carlo simulations of Hoshiba et al. [1991] were simultaneously fit to the observed logarithmically averaged data using a 50% overlapping distance window of 5.0 km. Next, the averaged data, which consisted of 28 points evenly spaced between 2.5 and 70 km hypocentral distance, were used to compute the sum of squared residuals for models with various combinations of B_0 and L_e. Figure 5 is a representative residual map which shows the ratio of the sum of squared residuals relative to the minimum solution. Because we have overlapped our data by 50%, we have roughly 40 degrees of freedom for each model estimate. Using the F distribution at the 90% level of confidence, the ratio of two random variables each having 40 degrees of freedom is 1.51. The model parameters corresponding to the average B_0 and L_e within the range of acceptable solutions are listed in Table 1 along with the corresponding scattering, intrinsic, and total Q^{-1}. The model fitting is amazingly good for frequencies above 3.0 Hz, despite the fact that the model assumes a full space with uniform scattering and intrinsic Q^{-1} and constant velocity. At 6.0 Hz, there is some indication of discrepancy for the second time window at short distances for all three regions as well as the first time window, specifically for Hawaii and central California. At 1.5 and 3.0 Hz, the model fitting generally works but has difficulty in explaining simultaneously the whole distance range.

Energy curves for the first time window of the Hawaii data at 1.5 and 3.0 Hz strongly increase with hypocentral distance, time windows at 1.5 and 3.0 Hz is striking, but is consistent with previous observations on coda waves which show an anomalously slow coda decay rate in Hawaii [Koyanagi et al., 1992] as compared to central California [Phillips et al., 1988] and Long Valley [Mayeda et al., 1991b]. This extraordinary increase in normalized energy out to 70 km cannot be solely attributed to the aforementioned problems of non-homogeneous spatial distribution of coda energy since this will only cause a factor of two increase in normalized energy at 70 km distance. The strong increase in energy with distance for the first time window could be due to surface wave energy, P wave coda contamination as well as mode converted waves. As for the discrepancy of the second time window at short hypocentral distances, and first time window for Hawaii, there are several plausible reasons. First, anisotropic scattering coefficient due to strong layering, such as volcanic flows, may affect vertical ray paths for short distances more than ray paths

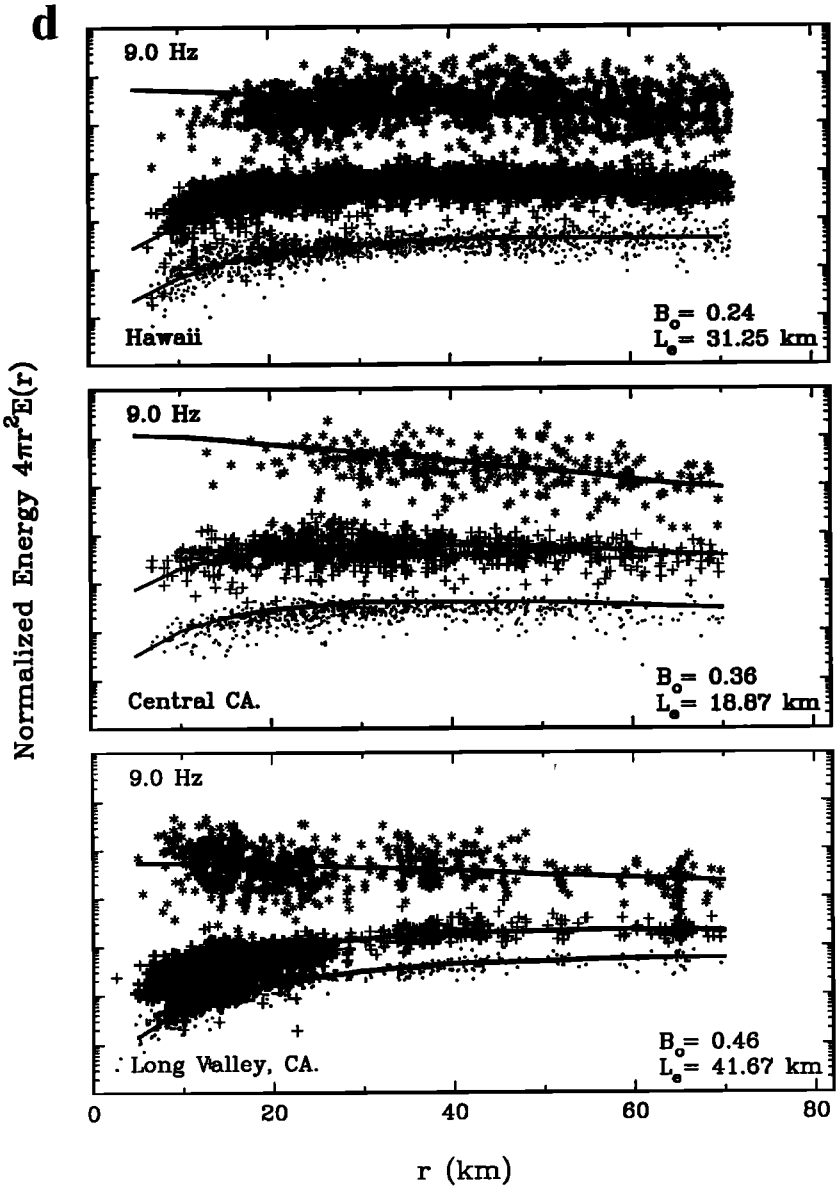

Fig. 4 (continued)

associated with larger station-receiver offsets. Furthermore, the depth of sampling at r = 70 km for the first time window is roughly equal to that of waves measured at r = 5 km for the second time window, independent of single or multiple scattering. Therefore, any depth-dependent scattering and intrinsic Q^{-1} in the lithosphere will cause the departure from the idealized uniform and homogeneous case. Though the lithosphere can be modeled well at high frequencies using this idealized model for all distances, we need to consider more complicated models to better understand the low frequency scattered waves. Also, a nonisotropic scattering pattern, such as strong backscattering, and trapped surface waves could be additional reasons for the discrepancy.

Interpretation

Figure 6 shows scattering Q^{-1}, intrinsic Q^{-1} and total Q^{-1} for all three regions as a function of frequency. To show the accuracy of the model fitting, the vertical error bars give the range of Q^{-1} at the 90% confidence level using the F distribution for 40 degrees of freedom. The strong frequency-dependent scattering Q^{-1} observed for all three regions is consistent with theoretical results [Wu, 1982; Sato, 1982; Frankel and Clayton, 1986] which predict that scattering Q^{-1} decreases with increasing frequency beyond the critical value corresponding to the dominant scale length of heterogeneity. Despite the rather large error bars we can make some general conclusions on the nature of attenuation in all three regions. In general, for frequencies less than or equal to 6.0 Hz, scattering Q^{-1} is greater than intrinsic Q^{-1}, whereas above 6.0 Hz the opposite is true. We found that in all three regions the scattering attenuation is strongly frequency dependent, decreasing proportional to f^{-1} to f^{-2} whereas intrinsic Q^{-1} is considerably less frequency dependent.

If scattering Q^{-1} decreases faster than f^{-1}, this is consistent with theoretical results for a medium characterized by Gaussian correlation function [Wu, 1982, Figure 2] when ka > 2, where ka is the normalized wavenumber and a is the correlation distance. When ka is large (i.e., ka »1), forward scattering is strong [Benites, 1990; Varadan et al., 1978]. Alternatively, if the dependence of scattering Q^{-1} on frequency is roughly f^{-1} this corresponds to a medium with exponential autocorrelation function or von Karman autocorrelation

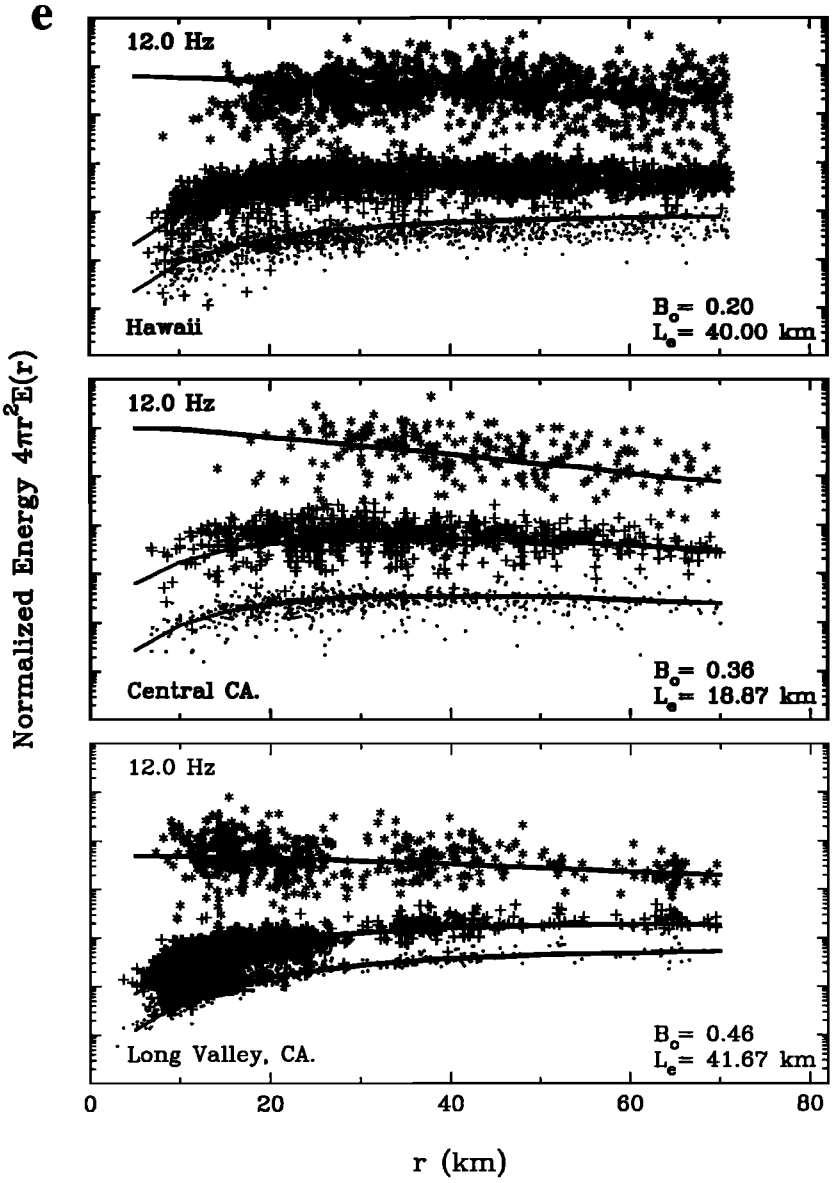

Fig. 4 (continued)

function of order $\nu = 0.5$ [Sato, 1982]. At high frequencies where the wavelength is much smaller than the dominant scale length of heterogeneity, forward scattering becomes important and thus applying an isotropic scattering model to a medium with relatively large forward scattering (e.g., $ka \gg 1$) will lead to an underestimation of B_0 since less energy will be scattered into the backward direction which affects energy in later time windows [Fehler et al., 1992]. Likewise, if the medium has stronger backscattering, B_0 will be overestimated. This may help to explain the high albedos at 1.5 and 3.0 Hz, especially for Hawaii. Though the fitting is generally poor at low frequency, the smaller separation of the three time windows, as compared with those greater than 3.0 Hz, also support that B_0 is higher than 0.5.

Comparison With Observed and Expected Coda Q

Coda Q^{-1} was computed for all three regions by fitting the single S to S back-scattering model of Aki and Chouet [1975] to the time-dependent amplitude of the S wave coda for lapse times much greater than twice the S wave travel time. Measurements of coda Q^{-1} in Hawaii and Long Valley become independent of station site for lapse times after roughly 30 s [Mayeda et al., 1991b; Koyanagi et al., 1992]. Therefore, we used a lapse time window from 30 to 60 s for our coda Q^{-1} analysis and averaged over all sites and events. As found in previous studies for these regions [Chouet, 1976; Phillips et al., 1988; Peng et al., 1987], coda Q^{-1} depends strongly on frequency and is remarkably unique to a particular region. Furthermore, coda Q^{-1} is not dependent on epicentral distances, at least less than 100 km. This is consistent with claims that coda Q^{-1} is a geophysical parameter which can be used to characterize the local and regional nature of the crust and upper mantle.

Recently, Zeng et al. [1991] have formulated an integral equation which gives the seismic energy density from a point source as a function of position and time for an unbounded medium characterized by constant velocity with uniform intrinsic and scattering Q^{-1}. The following equation is similar

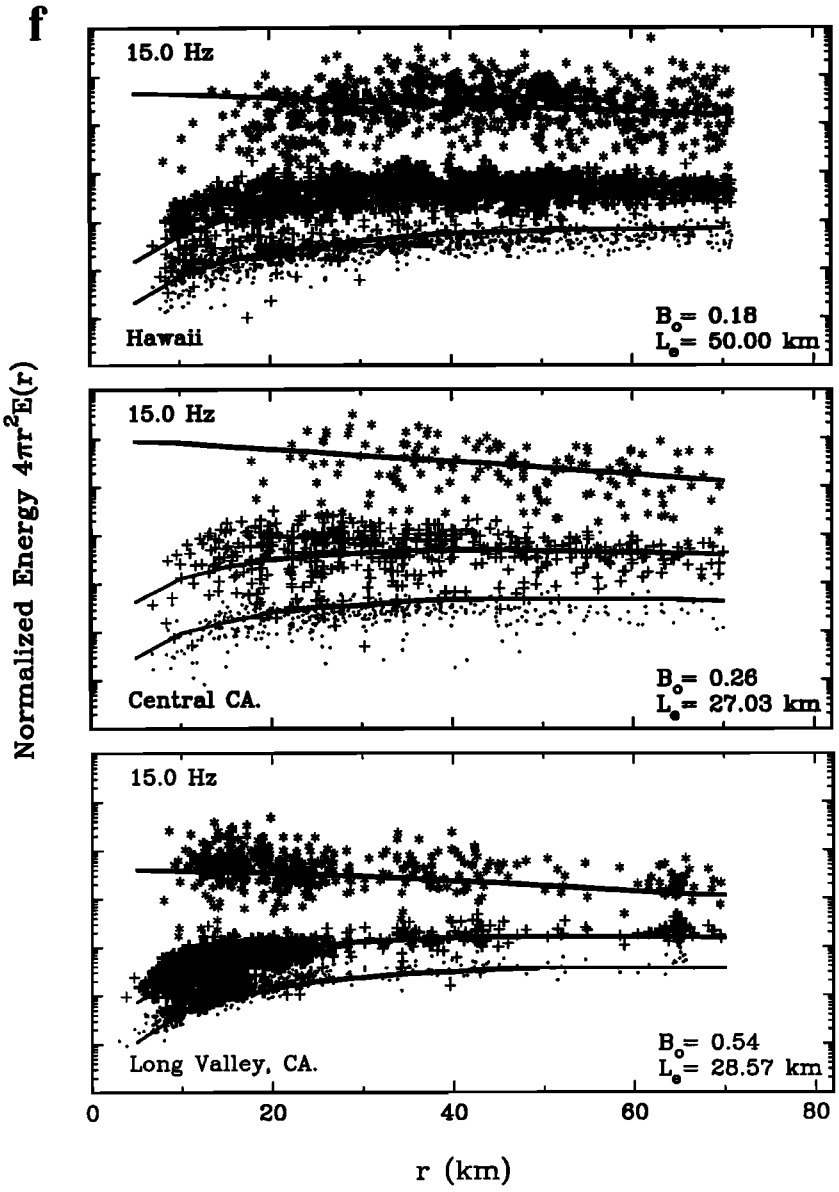

Fig. 4 (continued)

to the radiative transfer equation of Wu [1985]; however, Zeng et al. [1991] have solved the equation by including a time dependence. The equation below describes the complete multiple scattered energy at time t and source-receiver distance r for a medium with randomly distributed scatterers and uniform intrinsic attenuation in a full space,

$$E(r,t) = E_{in}\left(t - \frac{|r - r_0|}{v}\right) \frac{e^{-\eta |r - r_0|}}{4\pi |r - r_0|^2} + \int_V \eta_s E\left(r_1, t - \frac{|r_1 - r|}{v}\right) \frac{e^{-\eta |r_1 - r|}}{4\pi |r_1 - r|^2} dV_1 \quad (3)$$

where η_s is the scattering attenuation coefficient. The compact integral solution of (3) describes all orders of scattering for a medium with constant velocity v at position r and lapse time t.

$$E(r,t) = \frac{\delta\left(t - \frac{r}{v}\right) e^{-\eta v t}}{4\pi v r^2} + \sum_{n=1}^{2} E_n(r,t) + \int_{-\infty}^{+\infty} \frac{e^{i\omega t}}{2\pi} d\Omega \int_0^{\infty} \frac{\left(\frac{\eta_s}{k}\right)^3 \left[\tan^{-1}\left(\frac{k}{\eta + i\Omega/v}\right)\right]^4 \sin(kr)}{2\pi^2 v r \left[1 - \frac{\eta_s}{k} \tan^{-1}\left(\frac{k}{\eta + i\Omega/v}\right)\right]} dk \quad (4)$$

Zeng et al. [1991] demonstrated that the radiative transfer equation of Wu [1985] and the single and multiple scattering ray approaches used by Aki and Chouet [1975], Sato [1977], and Gao et al. [1983] among others are equivalent and can be derived from the above integral equation. Hoshiba [1991]

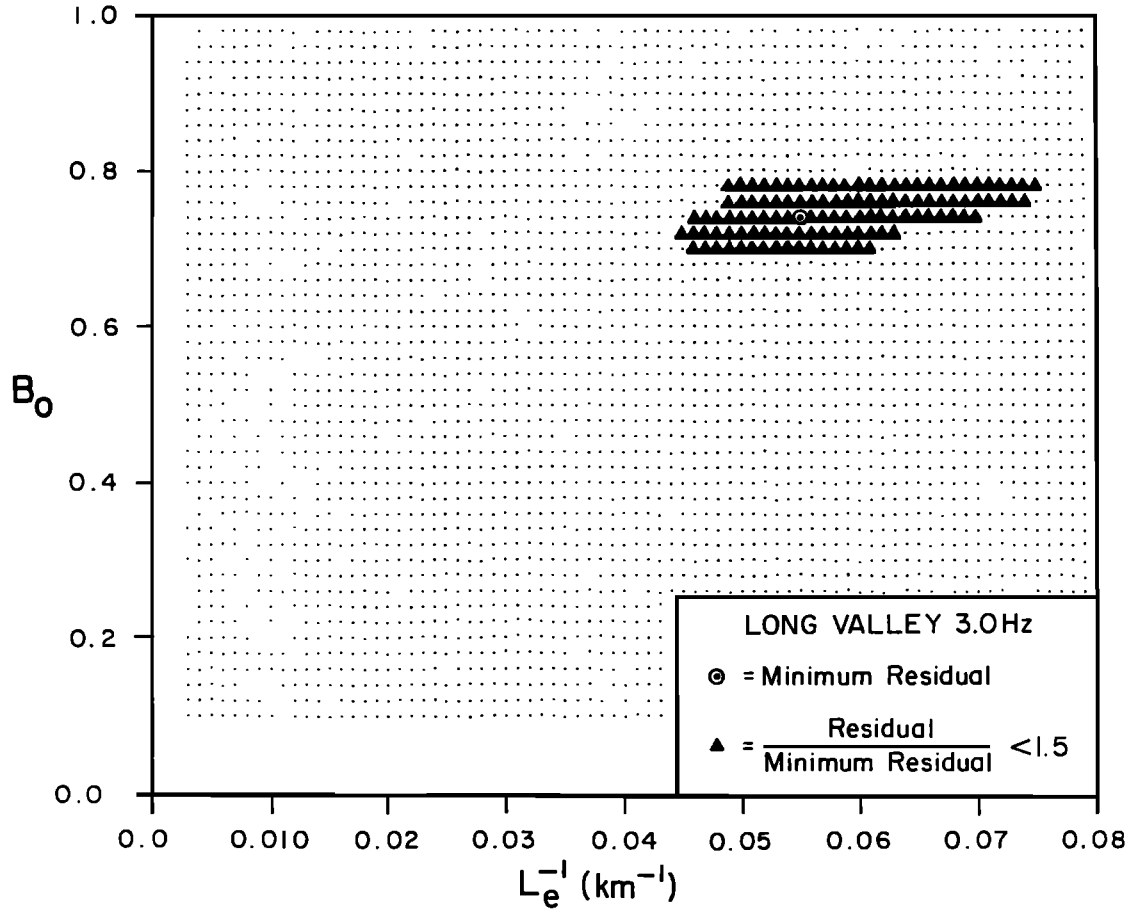

Fig. 5. Residual map for the 3.0-Hz Long Valley data. Each point is the ratio between the sum of squared residuals and the minimum solution. Triangles denote the 90% level of confidence using the F distribution for 40 degrees of freedom. The range of B_0 and L_e determine the vertical error bars in Figures 7a-7c.

TABLE 1. Range of Model Parameters and Corresponding Average Scattering, Intrinsic, and Total Attenuation, Q_s^{-1}, Q_i^{-1}, and Q_t^{-1}, Respectively

Frequency Hz	B_0	$\pm\delta B_0$	L_e^{-1}	$\pm\delta L_e^{-1}$	Q_s^{-1}	Q_i^{-1}	Q_t^{-1}	Coda Q^{-1}	
								Observed	Expected
				Long Valley, California					
1.5	0.85	0.03	0.0475	0.0045	0.01916	0.01312	0.02228	0.01250	0.00202
3.0	0.74	0.03	0.0555	0.0045	0.00903	0.00317	0.01220	0.00501	0.00227
6.0	0.55	0.02	0.0375	0.0025	0.00179	0.00179	0.00398	0.00202	0.00160
9.0	0.45	0.02	0.0230	0.0030	0.00081	0.00095	0.00177	0.00141	0.00081
12.0	0.47	0.02	0.0235	0.0015	0.00062	0.00070	0.00133	0.00119	0.00061
15.0	0.51	0.06	0.0300	0.0009	0.00064	0.00061	0.00125	0.00089	0.00056
				Central California					
1.5	0.76	0.05	0.038	0.0130	0.01275	0.00359	0.01634	0.01175	0.00359
3.0	0.63	0.03	0.035	0.0030	0.00598	0.00336	0.00934	0.00549	0.00240
6.0	0.39	0.04	0.045	0.0065	0.00181	0.00296	0.00477	0.00331	0.00279
9.0	0.37	0.02	0.055	0.0030	0.00135	0.00240	0.00375	0.00268	0.00226
12.0	0.38	0.03	0.054	0.0040	0.00085	0.00172	0.00257	0.00240	0.00159
15.0	0.28	0.05	0.040	0.0075	0.00051	0.00125	0.00176	0.00199	0.00110
				Hawaii					
1.5	0.98	0.02	0.042	0.0125	0.01854	0.00077	0.01931	0.01106	0.00102
3.0	0.98	0.02	0.030	0.0100	0.00677	0.00055	0.00732	0.00505	0.00049
6.0	0.43	0.06	0.042	0.0090	0.00185	0.00261	0.00446	0.00388	0.00236
9.0	0.25	0.05	0.033	0.0065	0.00058	0.00175	0.00233	0.00248	0.00163
12.0	0.20	0.05	0.026	0.0060	0.00031	0.00110	0.00141	0.00160	0.00101
15.0	0.18	0.05	0.020	0.0055	0.00016	0.00065	0.00081	0.00134	0.00066

$B_0 = \eta_s L_e$, where η_s is the scattering attenuation coefficient; $L_e^{-1} = \eta_e = (\eta_i + \eta_s)$, where η_i is the intrinsic attenuation coefficient and η_e is the total attenuation coefficient. Attenuation was determined by $Q_s^{-1} = \eta_s k^{-1}$, $Q_i^{-1} = \eta_s k^{-1}$ and $Q_t^{-1} = \eta_e k^{-1}$, where $k = 2\pi f/\beta$ and $\beta = 4.0$ km/s. The last two columns represent observed and expected coda Q^{-1} for all three regions using a lapse time window from 30 to 60 s.

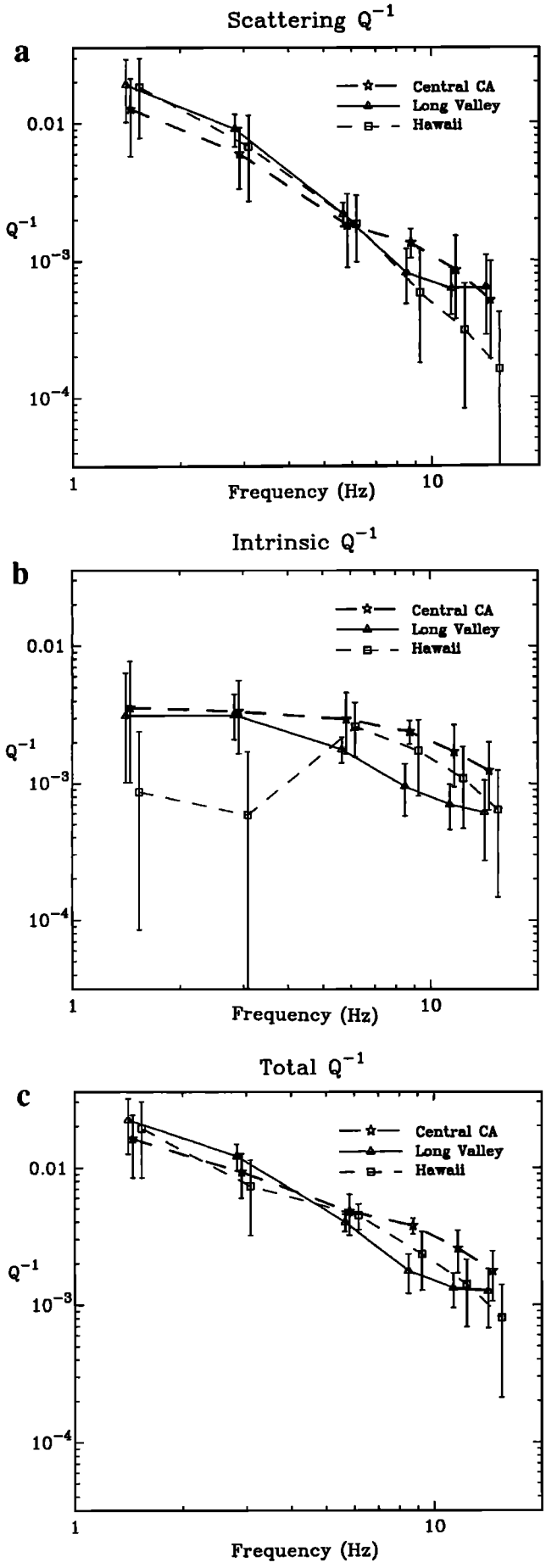

demonstrated the same equivalence by a Monte Carlo simulation. Using the integral equation of Zeng et al. [1991] and the model estimates listed in Table 1, we have determined the expected coda Q^{-1} by fitting the single-scattering formula of Aki and Chouet [1975] at a hypocentral distance of 10 km, roughly the same distance that was used in the observed coda Q^{-1} measurements. Figure 7 shows plots of expected and observed coda Q^{-1} along with the total Q^{-1} for all three regions. For both expected and observed coda Q^{-1} measurements, we used the same lapse time window, 30 to 60 s. From Table 1 and Figures 6 and 7 we clearly see that the expected coda Q^{-1} is nearly identical to the observed intrinsic Q^{-1}, in agreement with finite difference simulation results of Frankel and Wennerberg [1987] and laboratory experiments of Matsunami [1991]. However, the observed coda Q^{-1} in all three regions is intermediate between the total Q^{-1} and expected coda Q^{-1}, contradicting theoretical predictions. In general, for frequencies greater than or equal to 6.0 Hz, the model fitting is very good and thus the observed and expected coda Q^{-1} agree fairly well. From the analytic results of Shang and Gao [1988], we know that the coda Q^{-1} is identical to the intrinsic Q^{-1} for the two-dimensional case (i.e., when scatterers are randomly distributed and intrinsic Q^{-1} is uniform) and closer to the intrinsic Q^{-1} for the three-dimensional case [Gusev and Abubakirov, 1987]. The generally poor model fitting at low frequencies for the short distance range is equivalent to the discrepancy between observed and expected coda Q^{-1}. Recently, Y. Zeng (personal communication, 1991) has suggested that a depth-dependent intrinsic Q which increases with depth can explain the discrepancy between theoretical predictions and observations. He found that the observed coda Q^{-1} is closer to the total Q^{-1} (rather than intrinsic Q^{-1}) when the intrinsic Q^{-1} decreases with depth, even in strong scattering environments. In addition to the depth-dependent intrinsic Q^{-1}, the horizontal layering of crustal rocks may result in an anisotropic scattering coefficient g. The integral solution of Zeng et al. [1991] may provide the starting point for more realistic models, especially if nonisotropic scattering and heterogeneous distribution of scatterers and nonuniform absorption can be included.

Conclusion

In general, for frequencies less than or equal to 6.0 Hz, scattering Q^{-1} is greater than intrinsic Q^{-1}, whereas above 6.0 Hz the opposite was true. We found that in all three regions, the scattering Q^{-1} is strongly frequency dependent, decreasing inversely proportional to frequency or faster. This suggests that the heterogeneity responsible for scattering is at least comparable to the wavelength for the lowest frequencies studied, of the order of a few kilometers. The frequency-dependent scattering attenuation for these regions is consistent with theoretical results for media with random velocity fluctuations characterized by exponential and Gaussian autocorrelation functions which predict that scattering Q^{-1} decreases with increasing frequency.

The model fitting worked amazingly well at all distances for frequencies 6.0 Hz and above. At high frequencies the lithosphere in all three regions can be modeled very well by the simple assumptions of homogeneously distributed scatterers and uniform intrinsic Q^{-1} with constant velocity. At larger distances the scattered waves sample deeper and thus the assumption of homogeneous distribution of scatterers and uniform absorption is better. At short distances, the model

Fig. 6. (a) Scattering, (b) intrinsic, and (c) total Q^{-1} plotted for all three regions determined in this study (Table 1). In general, scattering Q^{-1} is the dominant mechanism for frequencies less than or equal to 6.0 Hz, whereas above 6.0 Hz, intrinsic Q^{-1} dominates over scattering Q^{-1}.

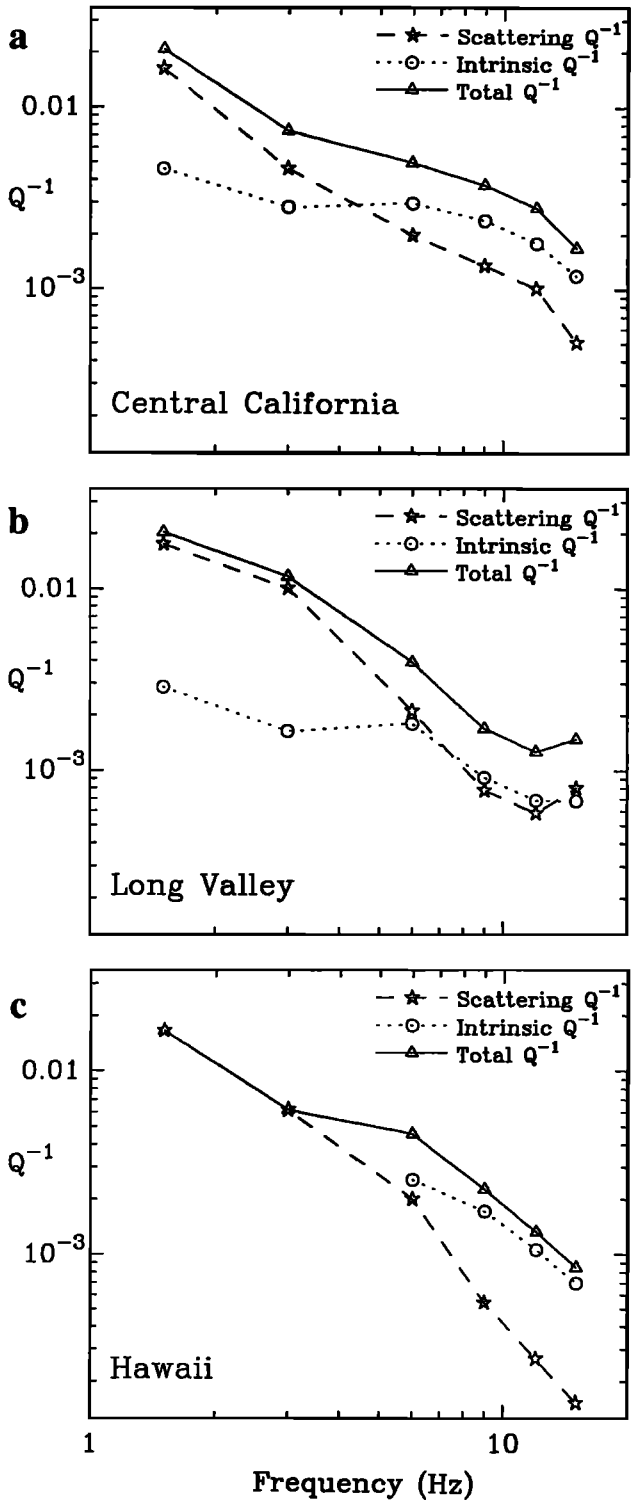

Fig. 7. Plots showing the total Q^{-1} along with expected and observed coda Q^{-1} for (a) central California, (b) Long Valley, and (c) Hawaii. Expected coda envelopes were generated by the integral equation of Zeng et al. [1991] using the model parameters listed in Table 1. The coda envelopes for both expected and observed data were fit to the single-scattering model of Aki and Chouet [1975] using a time window from 30 to 60 s. Notice that the observed coda Q^{-1} is intermediate between the total Q^{-1} and coda Q^{-1}, in disagreement with theory which predicts that coda Q^{-1} should be a measure of the intrinsic Q^{-1} [e.g., Frankel and Wennerberg, 1987].

fitting at low frequency is poor, perhaps due to complexities in the shallower part of the crust. These include anisotropic scattering coefficient, nonisotropic scattering pattern, or non-uniform absorption. At larger distances the first time window at low frequencies may be contaminated by surface waves and P wave coda. In addition to the possibility of nonisotropic scattering for all three regions, Long Valley may have additional complexities. The strong lithologic contrast between the caldera fill adjacent to crystalline rock [Hill, 1976] may violate our assumptions of constant velocity, homogeneously distributed scatterers and uniform intrinsic Q^{-1}. Models which incorporate heterogeneously distributed nonisotropic scatterers in a layered medium with depth-dependent intrinsic Q^{-1} are necessary to study more complex regions such as Hawaii and Long Valley.

The large discrepancy between observed and expected coda Q^{-1} at 1.5 and 3.0 Hz decreases sharply for frequencies 6.0 Hz and greater, where the model fitting for the observed energy-distance relation at multiple lapse time windows is significantly better. At low frequencies, complexities in the shallower crust are the cause for the poor fits at short distances, especially for the second time window. Though theoretical studies based on the models with uniform scatterers and constant intrinsic Q^{-1} predict that coda Q^{-1} should be closer to intrinsic Q^{-1}, the observed coda Q^{-1} is intermediate between the total Q^{-1} and expected coda Q^{-1} for an idealized case of uniform distribution of scatterers and homogeneous absorption which predict that coda Q^{-1} should be close to the intrinsic Q^{-1}. Heterogeneous models are necessary to explain observations at 1.5 and 3.0 Hz.

Acknowledgments. The authors are grateful to Jerry Eaton for his kind assistance in obtaining USGS station histories of calibration and gain for the Menlo Park seismic network. Comments by Anton Dainty and an anonymous reviewer helped greatly in our revision. In addition, the authors wish to thank the staff at the Hawaiian Volcano Observatory, especially Jennifer Nakata, who provided computer support for HVO data collection, clarification of station histories, HYPOINVERSE parameters, and digitized maps of the island of Hawaii. Special thanks also to Egill Hauksson, Rick Lester, Fred Klein, Paul Okubo, Wilfred Tanigawa, Tom English, and Robert Koyanagi for their logistical support and patience during various phases of our data collection. The model fitting to determine the best fitting model parameters was performed by Mitsuyuki Hoshiba. Kevin Mayeda has been supported by a doctoral fellowship from the Arco Oil foundation and Keiiti Aki has been supported under DOE grant DEFG03-87-ER-13807.

References

Abubakirov, I. R., and A. A. Gusev, Estimation of scattering properties of lithosphere of Kamchatka based on Monte-Carlo simulation of record envelope of a near earthquake, Phys. Earth Planet. Inter., 64, 52-67, 1990.

Aki, K., Attenuation of shear waves in the lithosphere for frequencies from 0.05 to 25 Hz, Phys. Earth Planet. Inter., 21, 50-60, 1980.

Aki, K., Summary of discussions on coda waves at the Istanbul IASPEI meeting, Phys. Earth Planet. Inter., 67, 1-3, 1991.

Aki, K., and B. Chouet, Origin of coda waves: Source, attenuation, and scattering effects, J. Geophys. Res., 80, 3322-3342, 1975.

Benites, R., Seismological applications of boundary integral and Gaussian beam methods, Ph.D. thesis, Mass. Inst. of Technol., Cambridge, 1990.

Chouet, B. A., Source, scattering, and attenuation effects on high frequency seismic waves, Ph.D. thesis, Mass. Inst. of Technol., Cambridge, 1976.

Eaton, J. P., Response arrays and sensitivity coefficients for standard configurations of the USGS short-period telemetered seismic system, U.S. Geol. Surv. Open File Rep., 80-316, 1980.

Fehler, M., M. Hoshiba, H. Sato, and K. Obara, Separation of scattering and intrinsic attenuation for the Kanto-Tokai region, Japan, using measurements of S wave energy vs hypocentral distance., Geophys. J. Int., in press, 1992.

Frankel, A. and R. W. Clayton, Finite difference simulations of seismic scattering: Implications for the propagation of short period seismic waves in the crust and models of crustal heterogeneity, J. Geophys. Res., 91, 6465-6490, 1986.

Frankel, A. and L. Wennerberg, Energy-flux model of seismic coda: Separation of scattering and intrinsic attenuation, Bull. Seismol. Soc. Am., 77, 1223-1251, 1987.

Gao, L. S., L. C. Lee, N. N. Biswas, and K. Aki, Comparison of the effects between single and multiple scattering on coda waves for local earthquakes, Bull. Seismol. Soc. Am., 73, 377-390, 1983.

Gusev, A. A., and I. R. Abubakirov, Monte-Carlo simulation of record envelope of a near earthquake, Phys. Earth Planet. Inter., 49, 30-36, 1987.

Hill, D. P., Structure of Long Valley caldera, California, from a seismic reflection experiment, J. Geophys. Res., 81, 745-753, 1976.

Hoshiba, M., Simulation of multiple scattered coda wave excitation based on the energy conservation law, Phys. Earth Planet. Inter., 67, 123-136, 1991.

Hoshiba, M., H. Sato, H., and M. Fehler, Numerical basis of the separation of scattering and intrinsic absorption from full seismogram envelope: A Monte-Carlo simulation of multiple isotropic scattering, Pap. Meteorol. Geophys., 42, 65-91, 1991.

Ishimaru, A., Wave Propagation and Scattering in Random Media, vols. 1 and 2, Academic, San Diego, Calif., 1978.

Koyanagi, S., K. Mayeda, and K. Aki, Frequency-dependent site amplification factors using the S-wave coda for the Island of Hawaii, Bull. Seismol. Soc. Am., in press, 1992.

Matsunami, K., Laboratory tests of excitation and attenuation of coda waves using 2-D models of scattering media, Phys. Earth Planet. Inter., 67, 36-47, 1991.

Mayeda, K., F. Su, F, and K. Aki, Seismic albedo from the total seismic energy dependence on hypocentral distance in southern California, Phys. Earth Planet. Inter., 67, 104-114, 1991a.

Mayeda, K., S. Koyanagi, and K. Aki, Site amplification from S wave coda in the Long Valley Caldera region, California, Bull. Seismol. Soc. Am., 81, 2194-2213, 1991b.

McSweeney, T., N. Biswas, K. Mayeda, and K. Aki, Scattering and anelastic attenuation of seismic energy in central and south central Alaska, Phys. Earth Planet. Inter., 67, 115-122, 1991.

Nakata, J., R. Koyanagi, W. Tanigawa, and A. Tomori, Hawaii Volcano Observatory, summary 85 - seismic data January to December 1985, report, U.S. Geol. Surv., Reston, VA, 1987.

Peng, J. Y., K. Aki, B. Chouet, P. Johnson, W. H. K. Lee, S. Marks, J. T. Newberry, A. S. Ryall, S. Stewart, and D. M. Tottingham, Temporal change in coda Q associated with the Round Valley, California, earthquake of November 23, 1984, J. Geophys. Res., 92, 3507-3526, 1987.

Phillips, W. S., The separation of source, path and site effects on high frequency seismic waves: An analysis using coda wave techniques, Ph.D. thesis, Mass. Inst. of Technol., Cambridge, 1985.

Phillips, W. S., W. H. K. Lee, and J. T. Newberry, Spatial variation of crustal coda Q in California, Pure Appl. Geophys., 128, 251-260, 1988.

Rautian, T. G., and V. I. Khalturin, The use of the coda for the determination of the earthquake source spectrum, Bull. Seismol. Soc. Am., 68, 923-948, 1978.

Sato, H., Energy propagation including scattering effects: Single scattering approximation, J. Phys. Earth, 25, 27-41, 1977.

Sato, H., Attenuation of S waves in the lithosphere due to scattering by its random velocity structure, J. Geophys. Res., 87, 7779-7785, 1982.

Sato, H., Temporal change in scattering and attenuation associated with the earthquake occurrence -- A review of recent studies on coda waves, Pure Appl. Geophys., 126, 465-498, 1988.

Shang, T. and L. Gao, Transportation theory of multiple scattering and its application to seismic coda waves of impulsive source, Sci. Sin., Ser. B, 31, 1503-1514, 1988.

Singh, S., and R. B. Herrmann, Regionalization of crustal coda Q in the continental United States, J. Geophys. Res., 88, 527-538, 1983.

Taylor, S., B. Bonner, and G. Zandt, Attenuation and scattering of broadband P and S waves across North America, J. Geophys. Res., 91, 7309-7325, 1986.

Toksöz, M., A. Dainty, E. Reiter, and R. S. Wu, A model for attenuation and scattering in the Earth's crust, Pure Appl. Geophys., 128, 81-100, 1988.

Varadan, V. K., V. V. Varadan, and Y. H. Pao, Multiple scattering of elastic waves by cylinders of arbitrary cross section, I, SH waves, J. Acoust. Soc. Am., 63(5), 1310-1319, 1978.

Wu, R. S., Attenuation of short-period seismic waves due to scattering, Geophys. Res. Lett., 9, 9-12, 1982.

Wu, R. S., Multiple scattering and energy transfer of seismic waves -- Separation of scattering effect from the intrinsic attenuation, I, Theoretical modeling, Geophys. J. R. Astron. Soc., 82, 57-80, 1985.

Wu, R. S., and K. Aki, Multiple scattering and energy transfer of seismic waves -- Separation of scattering effect from intrinsic attenuation, II, Application of the theory to Hindu Kush region, Pure Appl. Geophys., 128, 49-80, 1988.

Zeng, Y., F. Su, and K. Aki, Scattering wave energy propagation in a medium with randomly distributed isotropic scatterers, 1, Theory, J. Geophys. Res., 96, 607-619, 1991.

K. Aki, Department of Geological Sciences, University of Southern California, Los Angeles, CA 90089-0740 (FAX: 213-740-8801).

M. Hoshiba, Meteorological Research Institute, Nagamine 1-1, Tsukuba-shi, Ibaraki-ken, 305, Japan (FAX: 011-81-298-51-3730).

S. Koyanagi, NEIC, MS 967, Denver Federal Center, Box 25046, Denver, CO 80225.

K. Mayeda, Lawrence Livermore National Laboratory, Earth Sciences Dept. L-202, Livermore, CA 94550.

Y. Zeng, Department of Geological Sciences, University of Nevada, Reno, NV 89557.

(Received August 2, 1991;
revised November 12, 1991;
accepted December 5, 1991.)